

Expanded View Figures

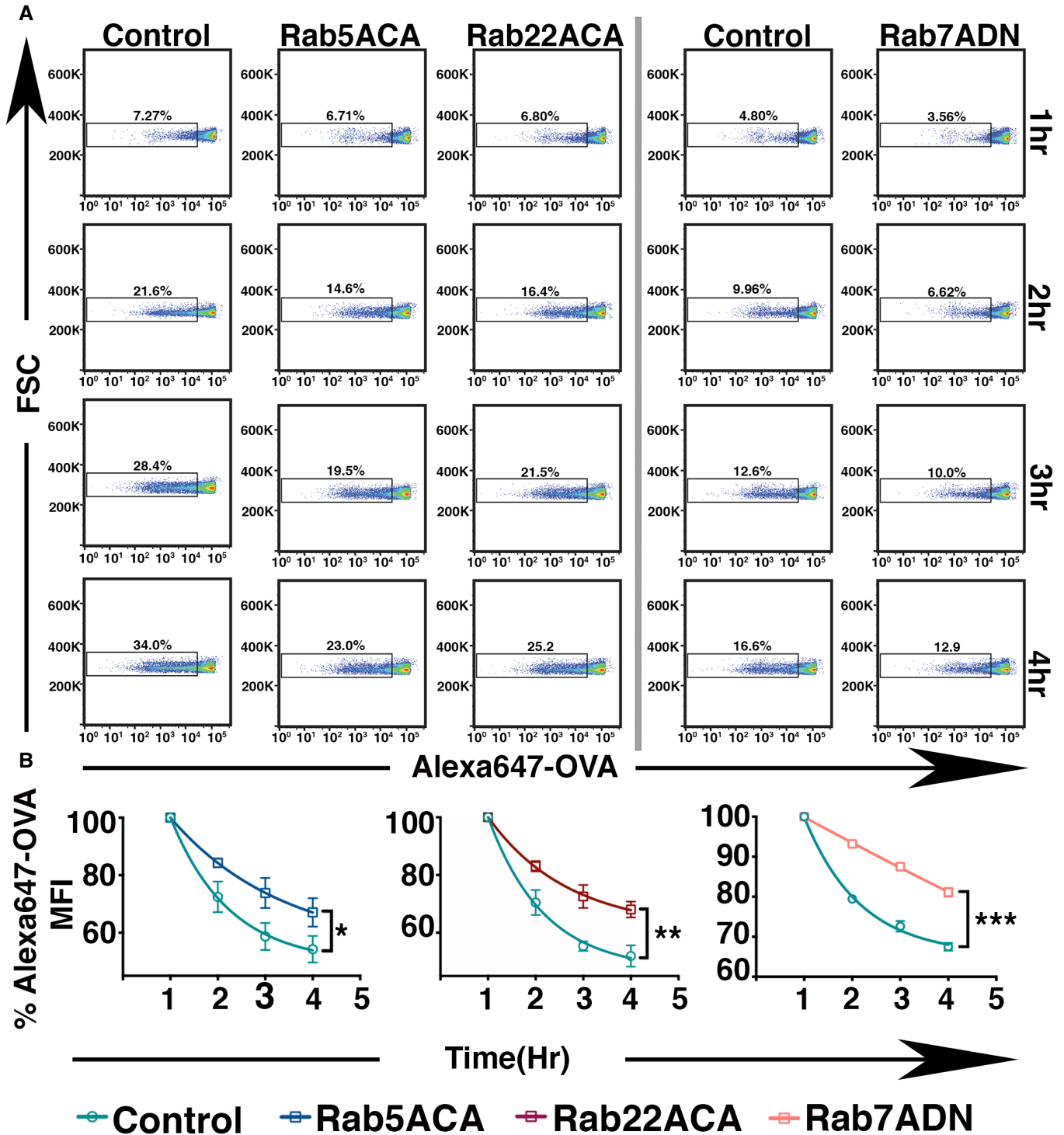


Figure EV1.

Figure EV1. Expression of Rab5ACA, Rab22ACA, and Rab7ADN restricts the degradation of phagocytosed antigen.

A Phagocytosed latex beads covalently conjugated with Alexa 647-OVA were extracted from BMDC expressing GFP or GFP-Rab5ACA or GFP-Rab22ACA or Rab7ADN at 1-h intervals, and analyzed for the loss of Alexa 647 fluorescence by flow cytometry.

B The mean Alexa 647 fluorescence on the beads normalized to the fluorescence at the 1-h time point is plotted ($n = 3$).

Data representation: In (A), a representative of three independent experiments is shown. In (B), the mean (\pm SEM) is plotted and analyzed by non-linear one-phase decay curve. The $t_{1/2}$ obtained from the above analysis was compared. * $P < 0.05$. ** $P < 0.01$, and *** $P < 0.005$ (one-way ANOVA).

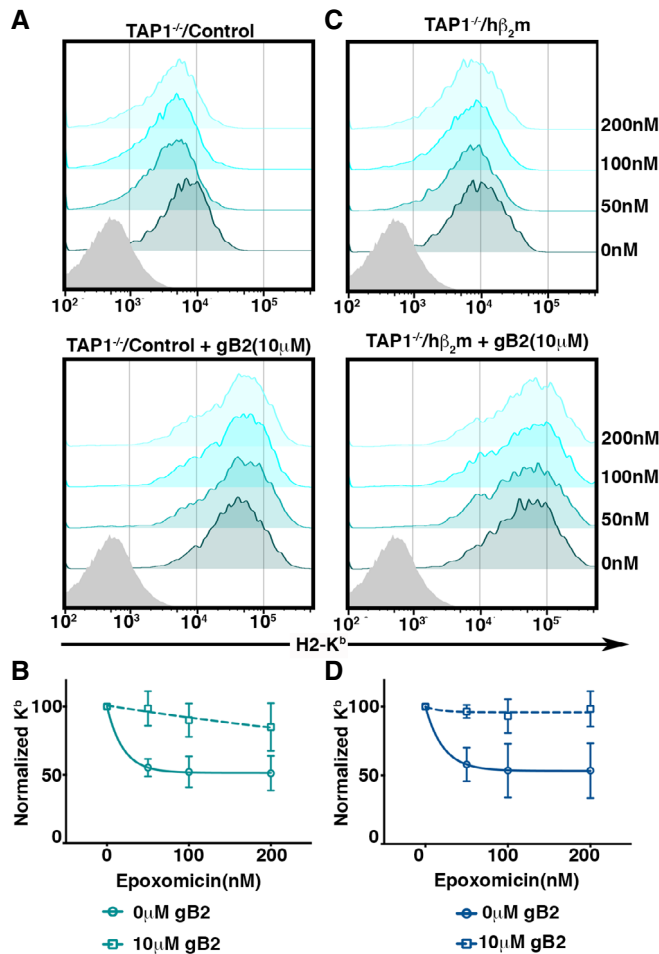


Figure EV2. Rescue of epoxomicin-mediated down-regulation of surface K^b by HSV-gB peptide.

A–D Cell surface K^b expression of TAP1^{-/-} BMDC transduced with control vector (A) or hβ₂m expressing vector (C), incubated with varying doses of epoxomicin in the presence and absence of 10 μM gB peptide, was analyzed by flow cytometry. (B, D) Mean (\pm SEM) surface K^b levels normalized to untreated cells were plotted ($n = 2$).

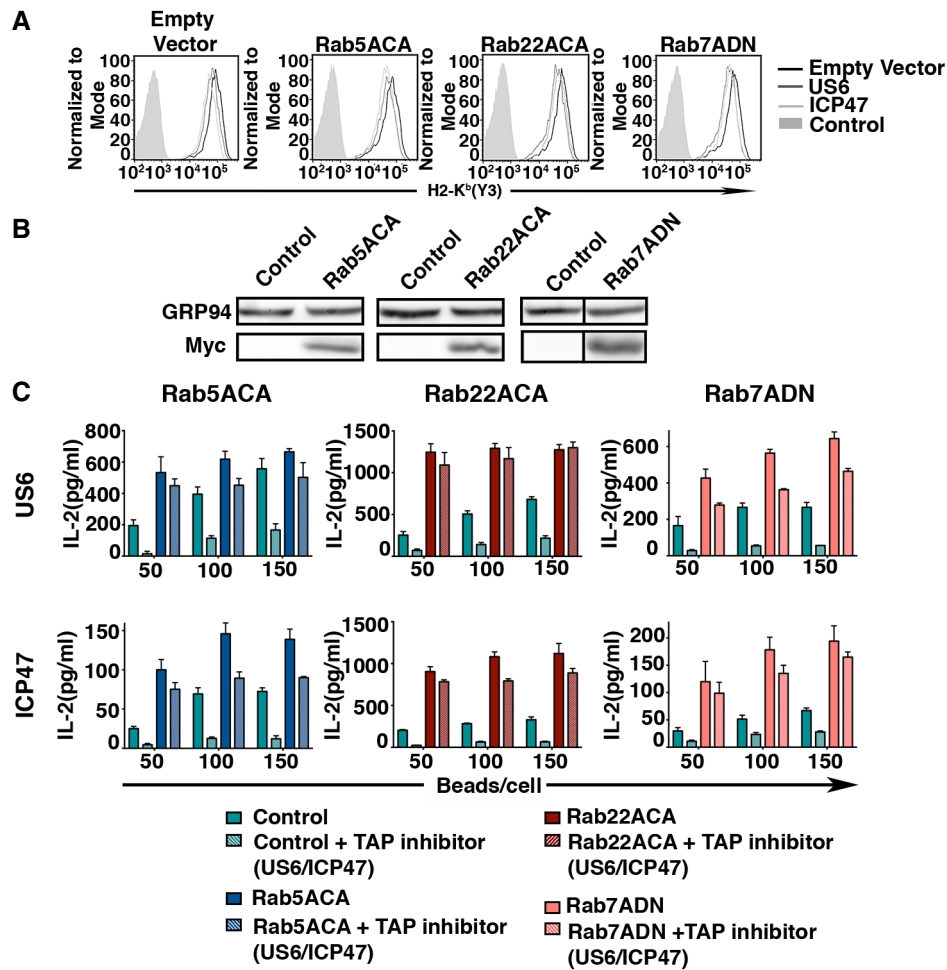


Figure EV3. Expression of Rab mutants in 293T-FcR-K^b and impact of co-expression of US6 or ICP47 with Rab mutants of the cell surface H2-K^b and cross-presentation.

A H2-K^b on the cell surface of 293T-FcR-K^b co-expressing US6 or ICP47 along with Rab mutants was measured by flow cytometry.

B Transient expression of Rab5ACA, Rab22ACA, and Rab7ADN in 293T-FcR-K^b was evaluated by immunoblotting with anti-Myc.

C Representative plots of at least three independent experiments of 293T-FcR-K^b cells co-expressing US6 or ICP47 with LacZ or Rab mutants were incubated with opsonized OVA-coated latex beads for 12 h. The effect of US6 or ICP47 along with the Rab mutants on cross-presentation was assessed by paraformaldehyde fixation and measuring IL-2 production by added B3Z cells. The assay was set up in triplicates, and the mean (±SD) of the triplicates is plotted.

Source data are available online for this figure.

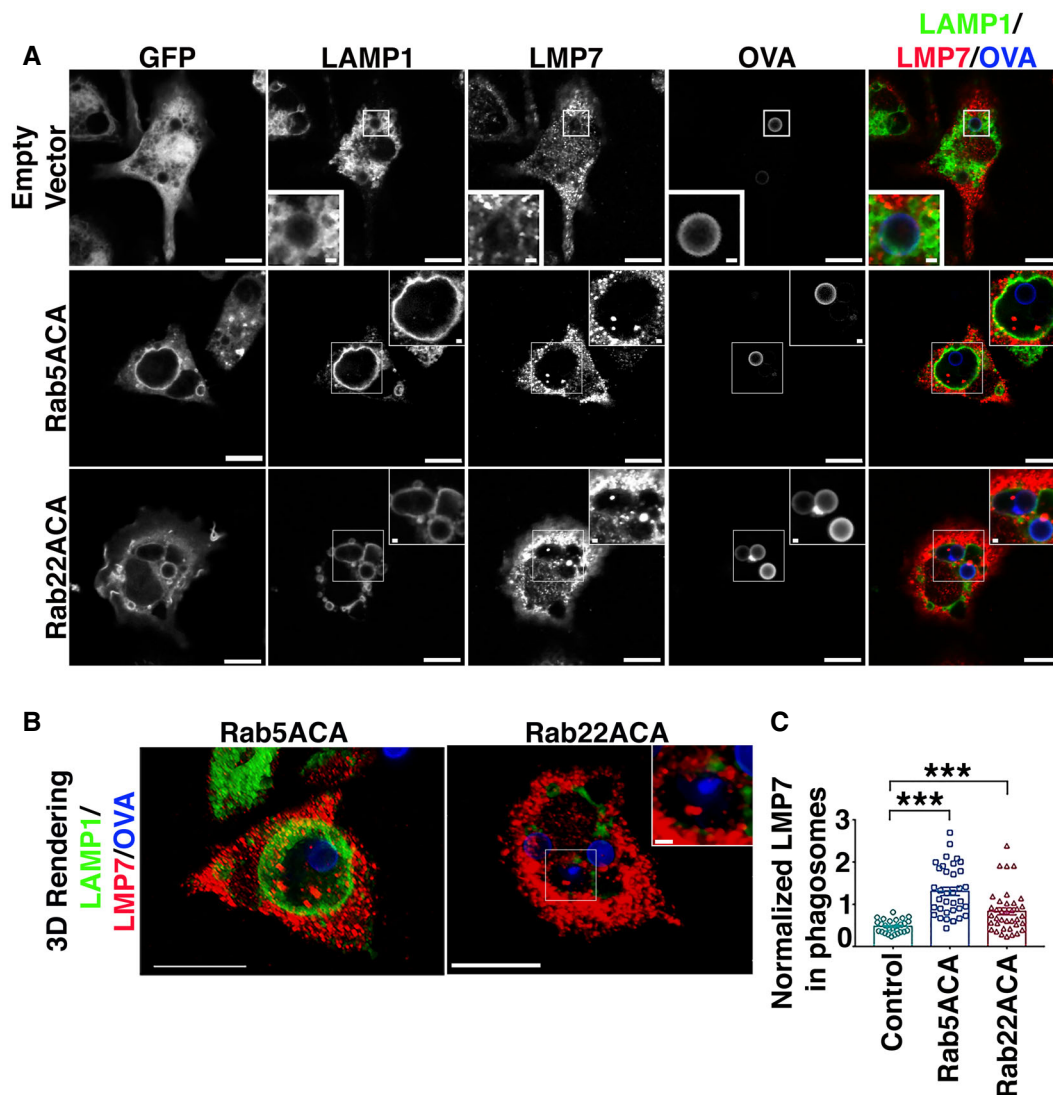


Figure EV4. Immunofluorescence analysis of localization of immunoproteasome subunit, LMP7, with respect to phagosomal lumen.

A, B BMDCs expressing GFP, GFP-Rab5ACA, or GFP-Rab22ACA were stained for LMP7 and LAMP1, and analyzed by confocal microscopy (A, B), 4 h after uptake of Alexa 647-OVA-coated bead. A single optical section (A) and a 3D-rendering (B) of 10 optical sections of a representative cell are shown (Bar 10 μ m). White rectangle boxes marking the regions of interest containing LAMP1-positive vacuole containing beads coated with Alexa 647-conjugated OVA are magnified as inset (Scale bars = 1 μ m).

C The same cells were analyzed for LMP7 fluorescence intensity within the phagosomal lumen as defined by a region of interest positive for Alexa 647-OVA enclosed within a limiting membrane positive for LAMP1. The fluorescence intensity of LMP7 within the phagosomal lumen normalized to Alexa 647-OVA was calculated, and the data from 3 ($n = 3$) independent experiments were compiled and plotted (C). At the least 28 transduced BMDC, cells were analyzed for each transduction and each cell is represented as a data point.

Data information: In (C), the mean (\pm SD) was plotted. Individual circles represent the analysis of an individual cell. *** $P < 0.005$.